NJC

Accepted Manuscript

ROYAL SOCIETY OF CHEMISTRY

www.rsc.org/njc

New Journal of Chemistry

ARTICLE

Research on the influence of alkyl ammonium bromides on the properties of Ag/AgBr/GO composites

Shuang Wang,[a] Chun Liu,[b] Leizhi Zheng,[b] Changqing Lin,[b] Pengpeng Kuang,[c] Xiaoqi Fu,*[a,c] Naichao Si*[a]

Silver/silver halides/graphene oxide (Ag/AgX/GO) plasma resonance photocatalysts have received extensive attention due to their excellent photocatalytic activities in the visible-light region. From a synthetic point of view, it is highly attractive to investigate the influence of synthesis conditions on the properties of Ag/AgX/GO, such as halide source, metal precursor and pH value. We present a water/oil method of fabricating Ag/AgBr/GO nanostructures by using alkyl ammonium bromides with different carbon chain length as halide sources. The structural details and textural properties of these resultant Ag/AgBr/GO nanocomposites are characterized by X–ray diffraction, transmission electron microscopy, and X–ray photoelectron spectroscopy studies. The results show that the decompositions of AgBr to Ag accelerate when using the short carbon chain of alkyl ammonium bromide. Photocatalytic experiments show that the photocatalytic activities of Ag/AgBr/GO-CTAB and Ag/AgBr/GO-DTAB are higher than those of Ag/AgBr/GO-TBAB and Ag/AgBr/GO-TMAB. Raman scattering studies indicate that these resultant Ag/AgBr/GO nanocomposites can not only enhance the Raman signals of GO, but also be used as surface-enhanced Raman scattering (SERS) substrates to enhance the Raman signals of dye molecules. Their enhancement degrees are different when using different carbon chain of alkyl ammonium bromide. Owing to the high photocatalytic performance, chemical stability and SERS effect, Ag/AgBr/GO-CTAB and Ag/AgBr/GO-DTAB nanocomposites can be used as the recyclable SERS substrates.

Introduction

Titanium dioxide (TiO$_2$) has been extensively investigated as a typical semiconductor photocatalyst, due to its high photocatalytic activity, low cost and non-toxicity.[1–4] However, it can utilize no more than 5% of the total solar energy because of the wide band gap (~3.2 eV). Recently, considerable interest has been focused on investigating silver-based plasmon resonance photocatalysts, especially the silver/silver halides (Ag/AgX) photocatalysts, which possess excellent photocatalytic activity in the visible-light region.[5–9] Researches show that the Ag/AgX photocatalysts exhibit high absorption coefficients in a broad UV–vis spectral range due to the strong surface plasmon resonance (SPR) of silver nanoparticles. Moreover, silver nanoparticles can trap electrons during the separation of photo-generated electron–hole pairs and enhance photocatalytic efficiency.

Another way to improve photocatalytic efficiency is to load

photocatalysts onto a carrier. Graphene oxide (GO), a sp^2-bonded carbon sheet with a thickness of single atom, is an outstanding carrier, which provides abundant opportunities for the construction of GO-based photocatalysts.[10–14] Zhu et al.[15, 16] have prepared GO enwrapped Ag/AgX photocatalysts in oil/water and water/oil microemulsions by using cetyltrimethylammonium bromide (CTAB) as the halide source. They proposed that the enhanced photocatalytic performances of Ag/AgX after loading with GO is due to the hybridized GO acting as the electron-transfer medium to promote charge separation and transportation. Zhang et al.[17] also obtained similar result in GO grafted Ag@AgCl hybrid. However, in these cases, the most-used halide source is CTAB or cetyltrimethylammonium chloride (CTAC). As known, there are several kinds of alkyl ammonium halides, such as CTAB, dodecyltrimethylammonium bromide (DTAB), tetrabutylammonium bromide (TBAB), and tetramethylammonium bromide (TMAB). These alkyl ammonium halides with different carbon chain length would cause differences in their photocatalytic performances. Consequently, an investigation of the influence of the carbon chain length on the photocatalytic performance of Ag/AgX/GO is desired.

Furthermore, as we know, Ag nanoparticles can exhibit an optical phenomenon known as surface-enhanced Raman scattering (SERS) which can provide a spectral intensity often enhanced by many orders of magnitude for molecules adsorbed thereon.[18–20] The Ag nanoparticles on the surface of Ag/AgX/GO composites could also used for SERS detection. Therefore, an investigation of the

[a.] School of Material Science and Engineering, Jiangsu University, Zhenjiang 212013, P. R. China. E-mail: snc@ujs.edu.cn
[b.] Jingjiang college of Jiangsu University, Zhenjiang 212013, P. R. China.
[c.] School of Chemistry and Chemical Engineering, Jiangsu University, Zhenjiang 212013, P. R. China. E-mail: xfu@ujs.edu.cn
†Electronic Supplementary Information (ESI) available: The magnified XRD and XPS spectra. TEM images of Ag/AgBr/GOs after the photocatalytic degradation. Raman spectra of detection/light cleaning cycles of MO on the surface of Ag/AgBr/GO-DTAB, Ag/AgBr/GO-TBAB and Ag/AgBr/GO-TMAB.

influence of the carbon chain length of alkyl ammonium halide on the SERS effects is also desired.

In this study, Ag/AgBr/GO nanocomposites were synthesized by using alkyl ammonium bromides with different carbon chain length as halide sources. These as-synthesized Ag/AgBr/GO nanocomposites exhibited active photocatalytic activities under visible light irradiation, and well SERS effects. The influences of the carbon chain length of halide source on their photocatalytic performances and SERS effects were investigated.

Experimental section

Materials

Silver nitrate ($AgNO_3$) was purchased from Sigma-Aldrich Co. CTAB, DTAB, TMAB and TBAB were all analytical grade obtained from Sinopharm Chemical Reagent Co., Ltd. Natural graphite powder (44 μm) was provided by Qingdao Zhongtian Company. The other chemicals were all analytical grade without further purification.

Preparation of Graphene Oxide (GO)

GO was prepared from purified natural graphite by using a modified Hummers' method.[21] Typically, 1 g of graphite powder was added to 23 mL of cooled (0°C) concentrated H_2SO_4. 3 g of $KMnO_4$ was added gradually with stirring and cooling, the temperature of the mixture was maintained below 20°C. The mixture was then stirred at 35°C for 30 min. 46 mL of distilled water was slowly added to cause an increase in temperature to 98°C and the mixture was maintained at that temperature for 15 min. The reaction was terminated by adding 140 mL of distilled water followed by 1 mL of 30% H_2O_2 solution. The solid product was separated by centrifugation, washed repeatedly with 5% HCl solution until sulfate could not be detected with $BaCl_2$, then the suspension was dried in a vacuum oven at 60°C.

Synthesis of Ag/AgBr/GO

Ag/AgBr/GO nanocomposites were prepared by oil/water microemulsion method[15] with different alkyl ammonium bromides. 15 mg of the obtained GO powder was dispersed in 15 mL of water by sonication, forming stable GO colloid. After 30 min, 100 mL aqueous solution of 7.5×10^{-3} M $AgNO_3$ were added to the graphene oxide colloid solution with magnetic stirring for 30 min. 15 mL chloroform solution of 1.0×10^{-2} M alkyl ammonium bromide (CTAB, DTAB, TBAB, and TMAB) was added dropwise into the above mixture. Subsequently, the mixture was heated to 40°C and aged at that temperature for 0.5 h. The Ag/AgBr/GO samples can be obtained by centrifugation of the mixture and washed first with ethanol and then with deionized water by repeating centrifugations. The obtained Ag/AgBr/GO samples were labeled as Ag/AgBr/GO-CTAB, Ag/AgBr/GO-DTAB, Ag/AgBr/GO-TBAB, and Ag/AgBr/GO-TMAB, respectively.

Photocatalytic Performance

Typically, 50 mg Ag/AgBr/GO-CTAB was dispersed into a 100 mL aqueous solution of Methyl Orange (MO, 25 mg/L). Prior to irradiation, the dispersion was kept in the dark with magnetic stirring for 20 min to establish an equilibrium adsorption state. A 250 W Xe arc lamp equipped with a UV cutoff filter (λ>400 nm) used as the light source. Air was bubbled through the reaction solution from the bottom with an air flow of 250 mL/min to ensure effective dispersion. To monitor the degradation of MO, 3 mL of dispersion were taken out from the reaction system at certain time intervals and separated through centrifugation, and then monitored by UV–vis spectroscopy through recording the absorbance of the characteristic peak of MO at 464 nm. For comparison, the photocatalytics performances of Ag/AgBr/GO-DTAB, Ag/AgBr/GO-TBAB, and Ag/AgBr/GO-TMAB were investigated under the same condition.

SERS Spectra Measurement

In order to record the Raman spectra of MO on the surface of Ag/AgBr/GOs, an aliquot of 1 mL Ag/AgBr/GOs dispersion was dropped onto a Si wafer. After evaporation of the solvent, the samples were measured.

For SERS detecting of dye molecules, 10 mg Ag/AgBr/GO was dispersed in 20 mL MO (1×10^{-5} M) solution in the dark for 2 h in order to ensure that the adsorption equilibrium was reached. Then, 1 mL of the above mixture was dropped onto a Si wafer. The dropped solution was spread evenly into a circle and dried to form a thin film on the Si wafer. SERS measurements were taken on a Thermo Fisher spectrometer.

To measure the recyclable SERS detection ability of Ag/AgBr/GOs, after each SERS measurement, the above Si wafer was carefully immersed into water under a Xe lamp irradiation for 30 min and then rinsed to remove the residuals and dried with N_2 flow, and then Raman measured.

Characterization of Materials

X–ray diffraction (XRD) patterns of the nanocomposites were recorded on a Bruker D8 Advanced X–ray diffractometer using Cu–Ka radiation (k = 0.1542 nm). The diffraction data was recorded for 2θ angles between 5° and 80°. X–ray photoelectron spectra (XPS) recorded on a Thermo ESCALAB250 X–ray photoelectron spectrometer, using Al Kα (hυ=1486.6 eV). Morphology analyses of samples were carried out on a JEOL JEM–2100 transmission electron microscope (TEM). Photodegradation of MO was conducted by a light reactor (GHX–2) with a 250 W Xe arc lamp as the light source. Raman spectra were recorded on a Thermo Fisher spectrometer excited by a diode laser beam (532 nm, 1 mW) with an acquisition time of 2 s. For each sample, we took three SERS spectra in different position of the substrate and then averaged them.

Results and Discussion

Structure and Properties Characterization of Ag/AgBr/GO composites

XRD patterns of the resultant Ag/AgBr/GO samples are shown in Fig. 1. Their diffraction patterns look similar to each other with the same 2θ angles. The diffractions appearing at 26.7° (111), 30.9° (200), 44.4° (220), 52.6° (311), 54.9° (222), 65.2° (400) and 73.2° (420), correspond to the characteristic Bragg reflections of AgBr (JCPDS, 6-438). The existence of metallic Ag (JCPDS, 65-2871) could be confirmed by the other diffraction peaks at 38.2° (111), 44.4° (200) and 65.2° (220). The above result suggests the resultant AgBrs were essentially in a form of Ag/AgBr structure. The diffraction peaks of metallic Ag is very week, indicating the low weight contents of metallic Ag.[15, 17] It is worth to be noted that the relative intensities of Ag diffraction peaks increased when alkyl ammonium halide changed from CTAB to TMAB (ESI, Fig. S1). It indicates that the contents of metallic Ag decomposed from AgBr increased as the carbon chain of alkyl ammonium bromide shortened. Furthermore, as verified in researchers' works and our previous works[22, 23] that when GO is hybridized with inorganic particles, the regular layer structures of GO were usually disrupted, and the diffraction peak of

GO could hardly be observed. To further investigate the structures of Ag/AgBr/GO, morphologic analyses are carried out.
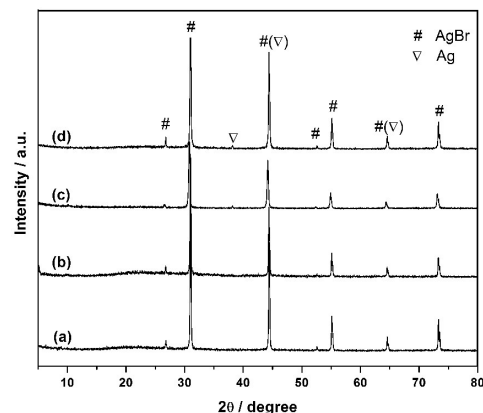

Fig. 1 XRD patterns of the resultant Ag/AgBr/GO composites: (a) Ag/AgBr/GO-CTAB, (b) Ag/AgBr/GO-DTAB, (c) Ag/AgBr/GO-TBAB, and (d) Ag/AgBr/GO-TMAB.
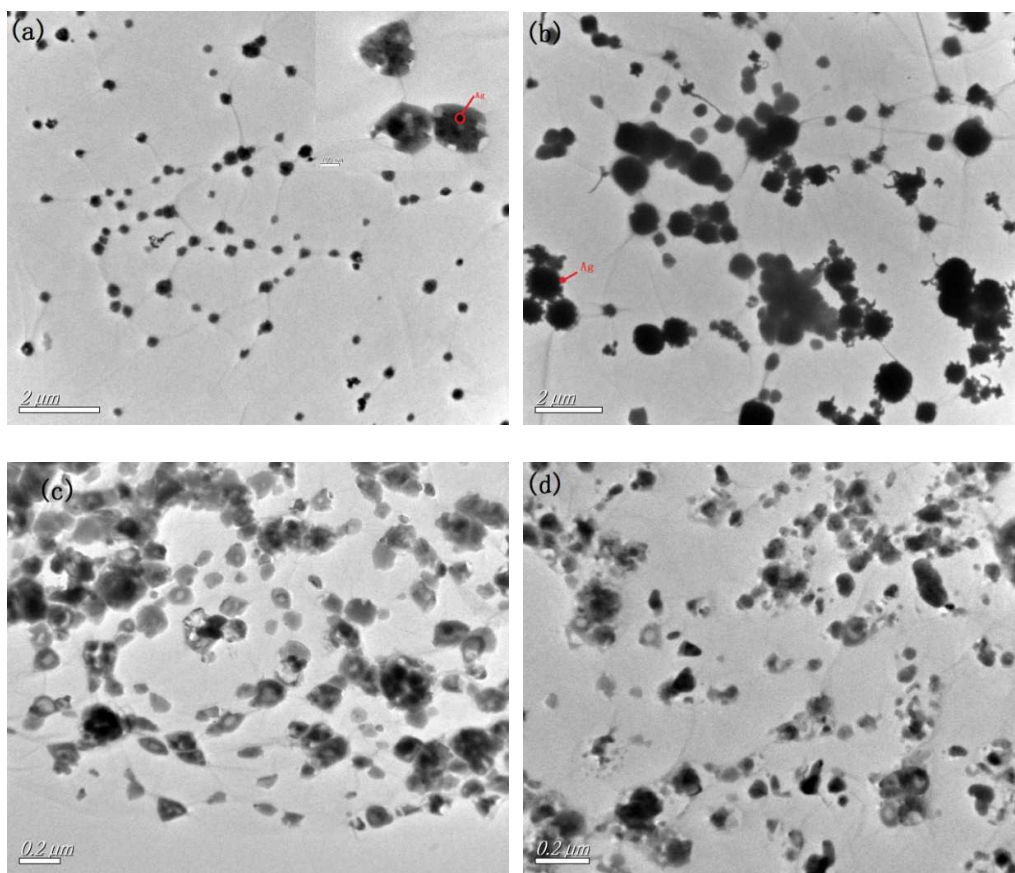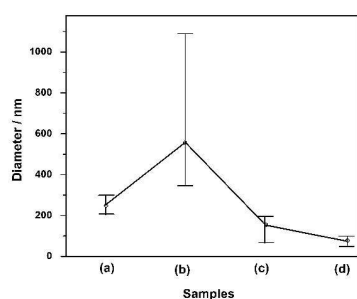

Fig. 2 TEM images of the resultant (a) Ag/AgBr/GO-CTAB, (b) Ag/AgBr/GO-DTAB, (c) Ag/AgBr/GO-TBAB, and (d) Ag/AgBr/GO-TMAB. The up insert is the magnified image.

Figure 2 displays TEM images of as-synthesized Ag/AgBr/GO samples. It is clearly seen that the almost transparent and crumpled silk-like GO sheets were decorated uniformly by AgBr naonospecies at each samples. From Fig. 2a, it can be seen that subround

morphologies of AgBr nanospecies with an average diameter of *ca.* 250 nm were well distributed on GO sheets. The up insert is the magnified image, in which some small nanoparticles (*ca.* 42 nm) adhered onto the surface of AgBr. This phenomenon also occurred

in three other samples. Combined with the above XRD analyses, we believe that the small nanoparticles were metallic Ag which were photoreduced from AgBr. The AgBr naonospecies were essentially Ag/AgBr nanoparticles. It's interesting that the size of Ag/AgBr particles is not linear with the carbon chain length of alkyl ammonium bromide. Fig. 3 depicts the relationship between the size of Ag/AgBr and the species of alkyl ammonium bromide. The size of Ag/AgBr nanoparticles first increased and then decreased, as the halide source changed from CTAB to TMAB. The largest average size of Ag/AgBr is about 550 nm for Ag/AgBr/GO-DTAB sample. Furthermore, it is worth mentioning that the decomposition degree of AgBr increased as the length of carbon chain shortened. The AgBr particles in Ag/AgBr/GO-CTAB show a slight decomposition, while a deep decomposition for Ag/AgBr/GO-TMAB. To further investigate the surface component variations of these Ag/AgBr based samples, XPS analyses are carried out.

Fig. 3 The calculated sizes of the resultant Ag/AgBr/GO composites: (a) Ag/AgBr/GO-CTAB, (b) Ag/AgBr/GO-DTAB, (c) Ag/AgBr/GO-TBAB, and (d) Ag/AgBr/GO-TMAB.
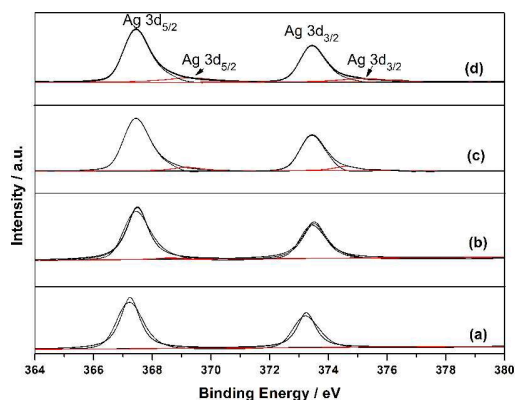

Fig. 4 XPS spectra of Ag 3d of the resultant Ag/AgBr/GO composites: (a) Ag/AgBr/GO-CTAB, (b) Ag/AgBr/GO-DTAB, (c) Ag/AgBr/GO-TBAB, and (d) Ag/AgBr/GO-TMAB.

X–ray photoelectron spectroscopy (XPS) of our Ag/AgBr/GO samples was examined in Fig. 4. As shown in Fig. 4a, the XPS spectra of Ag species of Ag/AgBr/GO-CTAB present two bands at ca. 367.5 and 373.4 eV, which can be ascribed to Ag $3d_{5/2}$ and Ag $3d_{3/2}$ binding energies, respectively.[15–17, 24] Each band of Ag element could further deconvoluted into two peaks, where the bands at around 367.2 and 373.2 eV are attributed to the Ag^+ of AgBr, and

those at about 368.2 and 374.3 eV are ascribed to the metallic Ag^0. It is interesting that the peak area of Ag^0 increased as using the short carbon chain of alkyl ammonium bromide (see the magnified XPS spectrum–ESI, Fig. S2). The calculated surface mole ratios of metallic Ag^0 to Ag^+ were 0.96:10, 1.38:10, 2.77:10, and 3.01:10 for Ag/AgBr/GO-CTAB, Ag/AgBr/GO-DTAB, Ag/AgBr/GO-TBAB, Ag/AgBr/GO-TMAB, respectively, indicating that much more AgBr is decomposed into metallic Ag when using the short carbon chain of alkyl ammonium bromide. This result is in good agreement with the TEM images, in which Ag/AgBr/GO-CTAB show a slight decomposition while a deep decomposition for Ag/AgBr/GO-TMAB.

Evaluation of Photocatalytic Activity

To evaluate the photocatalytic activity of the Ag/AgBr/GOs, the photodegradations of MO dye were carried out under visible light irradiation. The absorption spectral variations of MO during the photodegradation process are shown in Fig. 5. Evidently, MO is progressively degraded in the presence of Ag/AgBr/GOs, the concentration of MO decreases regularly, and the color of mixture gradually fades. It should be noted that no more than 15% of MO dyes are adsorbed on the Ag/AgBr/GOs hybrids under the dark reaction. For Ag/AgBr/GO-CTAB, about 66% of MO dyes are decomposed after irradiated for 40 min, while 79%, 27%, 20% degradations for Ag/AgBr/GO-DTAB, Ag/AgBr/GO-TBAB, Ag/AgBr/GO-TMAB, respectively. After being irradiated for 100 min, more than 90% of MO dyes are degraded for Ag/AgBr/GO-CTAB and Ag/AgBr/GO-DTAB samples, whereas only 36%, 25% of the dyes are degraded for Ag/AgBr/GO-TBAB and Ag/AgBr/GO-TMAB samples. The photocatalytic activities of Ag/AgBr/GO-CTAB and Ag/AgBr/GO-DTAB are clearly higher than those of Ag/AgBr/GO-TBAB and Ag/AgBr/GO-TMAB. Recently, Lou et al.[25] have used ionic liquids (CxMimCl, x = 4, 8, 12, 16) and AgNO₃ for fabricating AgCl photocatalysts, and found that carbon chain length had a great influence on the morphological structures. Long carbon chain tends to exhibit higher activity than that of short carbon chain. In our system, the similar result was found. However, it's interesting the photocatalytic performance of Ag/AgBr/GO-DTAB was slightly better than that of Ag/AgBr/GO-CTAB.
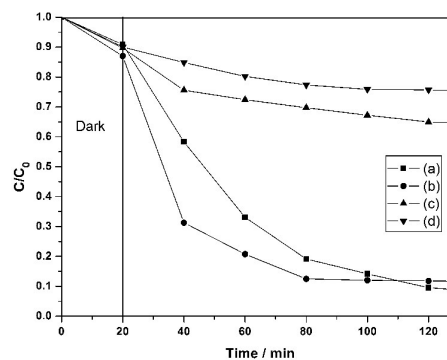
Fig. 5 Photocatalytic activities of (a) Ag/AgBr/GO-CTAB, (b) Ag/AgBr/GO-DTAB, (c) Ag/AgBr/GO-TBAB, and (d) Ag/AgBr/GO-TMAB composites for photodegradation of MO molecules under visible-light irradiation.

ARTICLE
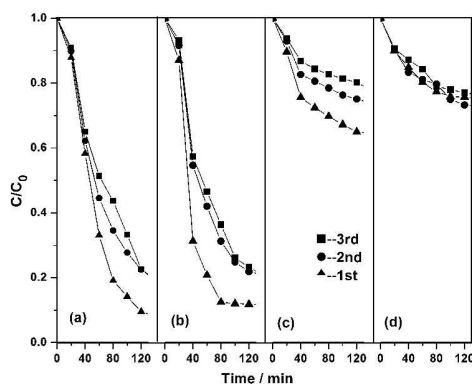
Fig. 6 Three consecutive cycling photodegradation curves of MO dye over (a) Ag/AgBr/GO-CTAB, (b) Ag/AgBr/GO-DTAB, (c) Ag/AgBr/GO-TBAB, and (d) Ag/AgBr/GO-TMAB composites, respectively.

The stabilities of these Ag/AgBr/GOs were further investigated by recycling these photocatalysts for MO degradation (Fig. 6). After three consecutive cycling photodegradation, the photocatalytic activities only showed a small decrease, but did not decrease significantly. The small decrease of the activity could be attributed to inevitable small amount loss of photocatalysts during the recycle process, and might also be due to the nice dispersibility of Ag/AgBr/GOs in aqueous solutions.[15, 26]

Wang et al.[27, 28] proposed that the stability of the Ag/AgX (X=Cl, Br) photocatalysts under light irradiation arise from the clusters of silver atoms around AgX surface which restrict the decomposition of AgX, in fact most likely from that a photon is absorbed by the Ag nanoparticles, and an electron separated from an absorbed photon remains in the nanoparticles rather than being transferred to the Ag^+ ions of the AgX lattice. In our system, the photoexcited electrons move to the surface of Ag and then transfer quickly to GO, and then trapped by O_2 in the solution to form superoxide ions (O_2^-) and other reactive oxygen species. The morphology of the Ag/AgBr/GOs did not display significant changes after three consecutive cycling photodegradation, as suggested by the TEM images (ESI, Fig. S3). It indicates that the resultant Ag/AgBr/GOs photocatalysts were stable under visible-light irradiation, which in good agreement with previous researchers' results.[15, 17, 25, 29]

In our system, silver nanoparticles can strongly absorb visible light because of their surface plasmon resonance (SPR). It widens the absorption range of AgBr. When Ag/AgBr/GOs subjected to visible light irradiation, they are excited due to the localized SPR of Ag nanoparticles and generate electron-hole pairs in Ag nanoparticles. Because the surface of AgBr particles is usually terminated by Br^- ion, free electrons in metallic Ag nanoparticle deposited on AgBr surface are polarized.[25] Under polarization field provided by AgBr core, the plasmon-excited electrons move to the surface of Ag and transfer quickly to GO, and then trapped by O_2 in the solution to form superoxide ions (O_2^-) and other reactive oxygen species, while holes transfer to the surface of AgBr, and then oxidize MO dyes.
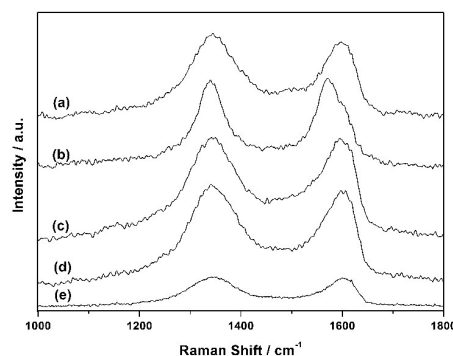
Fig. 7 Raman spectra of (a) Ag/AgBr/GO-CTAB, (b) Ag/AgBr/GO-DTAB, (c) Ag/AgBr/GO-TBAB, and (d) Ag/AgBr/GO-TMAB composites, and (e) GO nanosheets.

SERS Investigation of Ag/AgBr/GOs

The structures of these Ag/AgBr/GOs were further examined by Raman scattering. As known, noble metal (eg. Au, Ag, Cu)[30, 31] and some semiconductor (eg. AgX, TiO_2, α-Fe_2O_3)[32–35] nanoparticles can exhibit an optical phenomenon, surface enhanced Raman scattering (SERS), which provide a spectral intensity often enhanced by many orders of magnitude for molecules adsorbed thereon. Previous studies have shown that the Raman signals of GO/graphene attached to metallic nanostructures can be enhanced, which similar to the SERS effect.[23] We found that the resultant Ag/AgBr/GOs in our system also displayed SERS effect. In Fig. 7, we show the Raman spectra of these Ag/AgBr/GOs, together with the normal Raman spectrum of GO sheets. Obviously, the intensities of the D and G bands of GO increased at each spectrum of Ag/AgBr/GO sample in comparison with that of the original GO under the same test conditions. It is noted that the Raman enhancement shows a slight increasing trend as the halide source changes from CTAB to TMAB. The observed Raman enhancements in the present system can be attributed to surface plasmon resonance (SPR) enhancement induced by Ag nanoparticles and charge-transfer resonance (CT) enhancement involves the charge-transfer between GO and Ag/AgBr[23].
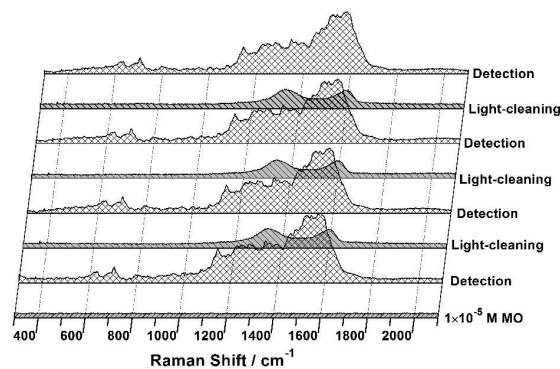
Fig. 8 Raman spectra of four detection/light cleaning cycles of MO on the surface of Ag/AgBr/GO-CTAB.

Table 1 Spectral lines and assignments of MO SERS bands.[41]

Spectral lines / cm^{-1}	Assignments
1586	υ(C-C)
1545	υ(C-C)
1526	υ(C-C)
1479	υ(C-N)
1457	υ(N=N) / δ(C-N)
1397	υ(N=N) / δ(C-N)
1368	υ(C-C)
1349	υ(C-N)
1296	β(C-H)
1280	β(C-H)$_{Me}$
1246	δ(C-C)
1226	δ(C-N)
1147	δ(C-C) / δ(C-N)
1081	δ(C-C)
1033	δ(C-C)
1005	ring breathing
954	
904	υ(C-C)
798	γ(C-H) / δ(C-C) / υ(C-C)
705	υ(C-N)$_{Me}$ / δ(C-C) / δ(C-N)
632	δ(C-C)

Note: υ, stretch; δ, deformation; β, in-plane-bend; γ, out-plane-bend.

Recently, Ag-GO based nanocomposites have been used as SERS substrates to enhance the Raman signals of probe molecules.[36–38] We found that the as-synthesized Ag/AgBr/GOs in our system also could be used as SERS substrates for detecting dyes molecules. Moreover, in the above discussion of photocatalytic performance, Ag/AgBr/GOs can photodegrade adsorbates into small inorganic molecules under visible light irradiation. Therefore, the as-synthesized Ag/AgBr/GOs substrates would be able to self-clean and reused for cycling SERS detection.[39, 40] Fig. 8 shows the SERS spectra of four detection/light cleaning cycles of MO solution on the Ag/AgBr/GO-CTAB substrate. It is clear that the Raman signals of MO (1×10^{-5} M) adsorbed on the Ag/AgBr/GO-CTAB substrate were enhanced remarkably, while MO solution without Ag/AgBr/GO-CTAB couldn't be detected at this concentration. Table 1 lists the Raman assignments of MO on the Ag/AgBr/GO-CTAB substrate. It should be noted that the enhanced Raman bands located in the range from 1000 to 1700 cm^{-1} show two blocks of background, which is similar to the D and G bands of GO/graphene. This is because the thin film of Ag/AgBr/GO-CTAB on the Si wafer has a certain thickness leads to strong peak intensities of D and G bands, and results in the Raman signals of MO appear on the shoulders of D and G bands. In the detection/light cleaning cycles, the Raman signal of MO almost completely vanished after visible light irradiation for 30 min, only left Raman signal of GO. The Raman signal of MO can be fully recovered after subsequent immersing of Ag/AgBr/GO-CTAB substrate into the MO solution again. The result was well reproduced after repeating the "detection/light cleaning" procedure four times. It indicates that Ag/AgBr/GO-CTAB is suitable for using as a recyclable SERS substrate. Similar result was obtained for Ag/AgBr/GO-DTAB substrate (ESI, Fig. S4). However, the Raman signal of MO on the surface of Ag/AgBr/GO-TBAB or Ag/AgBr/GO-TMAB was still remaining after visible light irradiation (ESI, Fig. S5, S6), which means they are not suitable for recycling SERS detection. This might be caused by that too much AgBr decompose to metallic Ag and the subsequent decrease of the photocatalytic performances of Ag/AgBr/GO-TBAB and Ag/AgBr/GO-TMAB.

Conclusions

In summary, Ag/AgBr/GO nanocomposites have been prepared using alkyl ammonium bromides with different carbon chain length as halide sources. The photocatalytic performances and Raman scattering properties of these Ag/AgBr/GO nanocomposites were correlated with the carbon chain length of alkyl ammonium bromide. Their photocatalytic activities became weaker when the length of the carbon chain became shorter, whereas an opposite change for their SERS enhancements. Furthermore, these Ag/AgBr/GO nanocomposites can not only enhance the Raman signals of GO, but also be used as SERS substrates to enhance the Raman signals of dye molecules. Owing to the high photocatalytic performance, chemical stability and SERS effect, Ag/AgBr/GO-CTAB and Ag/AgBr/GO-DTAB nanocomposites can be used as recyclable SERS substrates. This study may be helpful to controllable synthesis of graphene-based photocatalysts for desired structures and properties.

Acknowledgements

References

1 X. Chen and S. S. Mao, *Chem. Rev.*, 2007, **107**, 2891–2959.

2 U. Diebold, *Surf. Sci. Rep.*, 2003, **48**, 53–229.

3 R. Asahi, T. Morikawa, T. Ohwaki, K. Aoki and Y. Taga, *Science*, 2001, **293**, 269–271.

4 S. U. M. Khan, M. Al-Shahry and W. B. Ingler, *Science*, 2002, **297**, 2243–2245.

5 C. An, R. Wang, S. Wang and X. Zhang, *J. Mater. Chem.*, 2011, **21**, 11532–11536.

6 C. An, S. Peng and Y. Sun, *Adv. Mater.*; 2010, **22**, 2570–2574.

7 P. Wang, B. Huang, X. Qin, X. Zhang, Y. Dai, J. Wei and M. H. Whangbo, *Angew. Chem. Int. Ed.*, 2008, **47**, 7931–7933.

8 M. Zhu, P. Chen and M. Liu, *J. Mater. Chem.*, 2011, **21**, 16413–16419.

9 C. H. Zhang, L. H. Ai, L. L. Li and J. Jiang, *J. Alloy. Compo.*, 2014, **582**, 576–582.

10 Y. Y. Liang, H. L. Wang, H. S. Casalongue, Z. Chen and H. J. Dai, *Nano Res.*, 2010, **3**, 701–705.

11 J. Zhang, Z. Xiong and X. S. Zhao, *J. Mater. Chem.*, 2011, **21**, 3634–3640.

12 K. F. Zhou, Y. H. Zhu, X. L. Yang, X. Jiang and C. Z. Li, *New J. Chem.*, 2011, **35**, 353–359.

13 S. D. Perera, R. G. Mariano, K. Vu, N. Nour, O. Seitz, Y. Chabal and K. J. Balkus, *Acs Catal.*, 2012, **2**, 949–956.

14 N. Zhang, Y. H. Zhang, X. Y. Pan, X. Z. Fu, S. Q. Liu and Y. J. Xu, *J. Phys. Chem. C*, 2011, **115**, 23501–23511.

Journal Name ARTICLE

15 M. Zhu, P. Chen and M. Liu, *Acs Nano*, 2011, **5**, 4529–4536.

16 M. Zhu, P. Chen and M. Liu, *Langmuir*, 2012, **28**, 3385–3390.

17 H. Zhang, X. Fan, X. Quan, S. Chen and H. Yu, *Environ. Sci. Technol.*, 2011, **45**, 5731–5736.

18 J. F. Li, Y. F. Huang, Y. Ding, Z. L. Yang, S. B. Li, X. S. Zhou, F. R. Fan, W. Zhang, Z. Y. Zhou and D. Y. Wu, *Nature*, 2010, **464**, 392–395.

19 Z. Q. Tian, B. Ren and D. Y. Wu, *J. Phys. Chem. B*, 2002, **106**, 9463–9483.

20 H. X. Xu, J. Aizpurua, M. Kall and P. Apell, *Phys. Rev. E*, 2000, **62**, 4318–4324.

21 W.S. Hummers and R.E. Offeman, *J. Am. Chem. Soc.*, 1958, **80**, 1339–1339.

22 C. Xu, Y. Yuan, A. Cui and R. S. Yuan, *J. Mater. Sci.*, 2013, **48**, 967–973.

23 X. Fu, F. Bei, X. Wang, S. O'Brien and J.R. Lombardi, *Nanoscale*, 2010, **2**, 1461–1466.

24 D. Chen, T. Li, Q. Chen, J. Gao, B. Fan, J. Li, X. Li, R. Zhang, J. Sun and L. Gao, *Nanoscale*, 2012, **4**, 5431–5439.

25 Z. Z. Lou, B. B. Huang, P. Wang, Z. Y. Wang, X. Y. Qin, X. Y Zhang, H. F. Cheng, Z. K. Zheng and Y. Dai, *Dalton Trans.*, 2011, **40**, 4104–4110.

26 Y. Li and Y. Ding, *J. Phys. Chem. C* 2010, **114**, 3175–3179.

27 P. Wang, B. Huang, X. Qin, X. Zhang, Y. Dai, J. Wei and M. Whangbo, *Angew. Chem., Int. Ed.* 2008, **47**, 7931–7993.

28 P. Wang, B. B. Huang, X. Y. Zhang, X. Y. Qin, J. Hao, Y. Dai, Z. Y. Wang, J. Y. Wei, J. Zhan, S. Y. Wang, J. P. Wang and M. Whangbo, *Chem. Eur. J.* 2009, **15**, 1821–1824.

29 Z. Z. Lou, Z. Y. Wang, B. B. Huang and Y. Dai, *chemcatchem*, 2014, **6**, 2456–2476.

30 J. M. McLellan, A. Siekkinen, J. Y. Chen and Y. N. Xia, *Chem. Phys. Lett.*, 2006, **427**, 122–126.

31 Q. Yu and G. Golden, *Langmuir*, 2007, **23**, 8659–8662.

32 J. Wang, P. Zhang, T. He, H. Xin and F. Liu, *J. Phys. Chem.*, 1988, **92**, 1942–1945.

33 E. S. Brandt, *Appl. Spectrosc.*, 1993, **47**, 85–93.

34 A. Musumeci, D. Gosztola, T. Schiller, N. M. Dimitrijevic, V. Mujica, D. Martin and T. Rajh, *J. Am. Chem. Soc.*, 2009, **131**, 6040–6041.

35 X. Fu, F. Bei, X. Wang, X. Yang and L. Lu, *J. Raman Spectrosc.*, 2009, **40**, 1290–1295.

36 G. Lu, H. Li, C. Liusman, Z. Y. Yin, S. X. Wu and H. Zhang, *Chem. Sci.*, 2011, **2**, 1817–1821.

37 Z. Zhang, F. G. Xu, W. S. Yang, M. Y. Guo, X. D. Wang, B. L. Zhang and J. L. Tang, *Chem. Commun.*, 2011, **47**, 6440–6442.

38 J. Huang, L. M. Zhang, B. A. Chen, N. Ji, F. H. Chen, Y. Zhang and Z. J. Zhang, *Nanoscale*, 2010, **2**, 2733–2738.

39 X. Li, G. Chen, L. Yang, Z. Jin and J. Liu, *Adv. Funct. Mater.*, 2010, **20**, 2815–2824.

40 X. J. Zhang, J. H. Mei, D. D. Ni, Q. H. Guo, M. M. Xu, J. L. Yao and R. A. Gu, *Chem. J. Chinese U.*, 2011, **32**, 1563–1566.

41 B. Nandita and U. Siva, *J. Phys. Chem. A*, 2000, **104**, 2734–2745.

Graphical Abstract

The photocatalytic activities of as-synthesized Ag/AgBr/GO nanocomposites became weaker when alkyl chain became shorter, whereas an opposite change for their SERS enhancements.